Experimental investigation and annual performance mathematical-prediction on a novel LT-PV/T system using spiral-descent concentric copper tube heat exchanger as the condenser for large-scale application

Zhaomeng Li[1,2], Jie Ji[1*], Jing Li[2*], Xudong Zhao[2], Yu Cui[1], Zhiying Song[1], Xin Wen[1], TingTing Yao[1]

[1]*Department of Thermal Science and Energy Engineering, University of Science and Technology of China, 96 Jinzhai Road, Hefei, China, jijie@ustc.edu.cn*

[2]*Research Center for Sustainable Energy Technologies, Energy and Environment Institute, University of Hull, Hull, HU6 7RX, UK, jing.li@hull.ac.uk*

The condensers of loop thermosyphon PV/T systems (LT-PV/T) are usually integrated inside water tanks, which may bring some challenges during combination use. This research innovatively proposed a concentric copper tube heat exchanger as the condenser, which is combined with a copper tube evaporator beneath the absorber. The gaseous working fluid flows in the inner tube and the cooling water flows in the outer tube. Since ordinary water pipes are used for water circulating between the outer tube and water tank, this LT-PV/T collector can be used individually or combined with other collectors flexibly. To access its' performance, researches have been conducted: (1) Designing and fabricating the system prototypes; (2) Investigating system performance with different volume-filling ratios (26.5%, 34.8%, 43.2%); (3) Investigating the influences of working fluid (water, ethanol and R134A). (4) Evaluating the systems' performance with energy efficiency, exergy efficiency, and semi-empirical system efficiency models; (5) Conducting two case studies in South China (an individual collector & a 4 parallelly/serially-combined LT-PV/T collectors system). The system is first-of-its-kind and has obvious advantages in reliability, flexibility, space-saving and large-scale applications. The typical primary energy-saving efficiency of the LT-PV/T with R134a of 40% filling ratio can reach 78.0%, higher than the published LT-PV/T systems.

Keywords: loop thermosyphon, photovoltaic/thermal technology, concentric copper tube heat exchanger, working fluid, volume-filling ratio

Nomenclature

A	area, m^2	ζ	the coverage ratio of the PV cells, -
E	electrical output, W	η	efficiency, -
Ex	exergy, W	ξ	power generation efficiency in thermal power plants, -
G	solar radiation, W/m^2		
H	solar irradiation summation, KJ/m^2	*Subscripts*	
Q	solar heat gain, W	a	ambient environment
t	time, s	b	absorbing plate
T	temperature, K	f	primary energy-saving
U	energy loss coefficient, $KJ/(m^2 \cdot K)$	i	initial value of water tank of each interval
		pv	PV
Greek Symbols		tank	water tank
ε	exergy efficiency, -	th	thermal

1. Introduction

The photovoltaic efficiency of PV models typically drops by 0.2-0.5%/°C proportionally to the PV temperature climbing[1]. Solar hybrid photovoltaic/thermal (PV/T) technology integrates the PV cells and the solar thermal collector into one module to cool down the PV cells for better photovoltaic performance, and the superfluous thermal is utilized at the same time [2]. It can gain multiple kinds of energy on the facades or roofs of buildings with limited space. The advantage also lies in material cost-saving and simple installation. In the researches about PV/T technologies, water is widely chosen as the working fluid due to its high heat capacity, quickly cooling effect, as well as catering to residents' requirements for hot water. Though water-type based flat-plate PV/T[3] is the most used design for its simple fabricating, low material cost, and high electrical/thermal performance, it is faced with the risk of getting frozen in cold winter and thus the water pipes' cracking. Therefore, cooling channels like the gravity-assisted heat pipes[4] and micro-channel heat pipe array[5] have been researched in recent years. Specifically, the loop thermosyphon technology has also been applied in water heating systems [6], PV/T systems [7], or PV/solar-assisted heat pump water heating systems[8] for its advantage on anti-freezing of pipes, long-distance heat transference to heat storage tank, and temperature uniformity on PV [7, 9], though the published literature contains very few studies on PV/T. Basically speaking, loop thermosyphon pipe usually consists of 4 sections, viz. evaporating section, vapour line, condensing section and liquid line[10], sometimes the compensation chamber also included. So by separating the vapour lines and liquid lines, the loop thermosyphon pipes greatly minimized the entrainment between vapour and liquid flows in the traditional heat pipes, and thus reduce the pressure loss across the flow path[11].

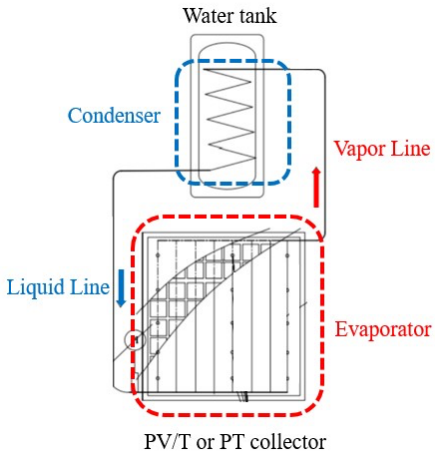

Fig. 1. Traditional LT condenser in water tank [12]

The condensing section of the loop thermosyphon pipes in PV/T, solar collector or solar-assisted heat pump system[13] is usually spiralled and immersed in a water tank[9], things like Fig.1. But considering the hot water demand of a house/building, a single LT-PV/T collector may be insufficient and several LT-PV/T collectors may need to be used in combination, in which case the adiabatic section (including the vapour line and liquid line) of each LT needs to be reconnected together. It is likely to be complex and challenging because of the high-quality requirements for the pipe welding, sealing, evacuating and working liquid rejecting for numbers of LT-PV/T cycling pipes. Worse, once sealing failure and working fluid leakage happens, though in just one LT-PV/T collector or anywhere of pipes, the whole joint-using system will stop work. And it's not easy to figure out exactly where goes wrong. What's more, how to ensure the liquified working fluid evenly flow back to the evaporation section of each loop thermosyphon in the complex line connection, and to prevent some evaporators from the insufficient quantity of working fluid in the evaporators, is also a concern.

To avoid these challenges, the novel LT-PV/T system in this research proposes to separate the condenser from the water tank. A concentric copper tube heat exchanger with a rectangular spiral descent act as the condenser of the loop thermosyphon instead, as shown in Fig.2. The working fluid of the loop thermosyphon flows inside the inner tube, releases heat, condenses and flows back to the evaporator through the liquid line. The cooling water driven by the water pump flows in the outer tube in the opposite direction against the working fluid, absorbs heat, and then flows back to the water tank and stores heat. As for the water pipes of each LT-PV/T, the reconnection is quite easy. Therefore, this kind of LT-PV/T can be used individually or be combined easily and flexibly depending on the domestic water requirement and the real spatial layout at the roof of the buildings, which means it is more spacing saving, more reliable and more suitable for large-scale systems. Also, by doing this, the vapour line and the liquid line are greatly lessened, reducing the flow resistance of the working fluid.

Another advantage lies in the unique rectangular spiral descent, which is more low-resistant for the liquefied working fluid flowing down and back, and the dimensions that match the width of the collector make it easy to save installation and using space. Furthermore, the circular copper tubes are laser-welded under the absorber plate as the evaporating section because it is technologically mature and the reliability can be guaranteed, which is also helpful to the popularization and application of LT-PV/T.

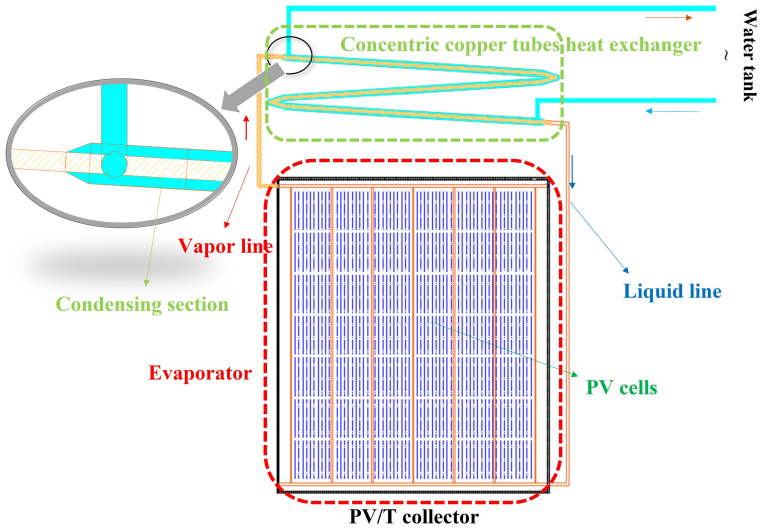

Fig. 2. The layout of the novel LT-PV/T

Though published studies about the application of loop thermosyphon pipes in the PV/T system are not too much, the existing literature can still inspire this research. Zhang et al. experimentally discussed the volume-filling ratio of isobutene (R600a) as working fluid in a traditional loop thermosiphon PV/T system with the heat flux and inclination and concluded that the optimum figure lay in between 32% and 40% for this structure[12]. Yu et al.[7] proposed a novel micro-channel loop heat pipe PV/T which used several microchannel heat pipes as evaporators and used a novel triple PCM heat exchanger as condenser. PCM is injected inside the outer tube to store the excess heat. R134a is chosen as working fluid flowing in the inner tube, releasing heat and flowing back to the liquid header and then flowing down to the mini channel evaporation pipes through some holes. The optimal refrigerant charge ratio of this system is concluded to be 30%. The thermal performance can be improved by decreasing inlet water temperature, speeding water flow, and enlarging the height difference between condenser and evaporator. Then Diallo et al.[14] proved that a larger packing factor and more microchannel heat pipes can benefit both the thermal and electrical performance of this system.

In addition, research about LT's characteristics and its' application in solar water heating systems or heat pump systems are of reference significance for this research. The heat transfer performance of loop thermosyphon is greatly affected by volume-filling ratio [15], tilt angle [12], heat flux [16], physical properties of the working fluid, geometrical and operational conditions[17] etc. Liu et al. [15] experimentally investigated the heat transfer in LHP with volume-filling ratios ranging from 38% to 87% overheat flux from 35 to 395 W/cm^{-2}. Results showed that the heat transfer ability was greatly better with the moderate filling ratios, though the pressure and temperature fluctuated obviously when the heat flux was high. Jiao et al. [18] theoretically discussed that the optimal filling ratio raised with increasing heat flux for a vertical two-phase closed thermosiphon. Huang et al. [19] experimentally found that the LHP-solar collector at 60% filling ratio performed better in thermal conversion. Arab et al. proposed to use pulsating heat pipes in solar water heating system and the distilled water as working fluid with 70% filling ratio showed to perform better[20]. A mixture of water and glycol is also used as the liquid within the loop thermosyphons for a solar water heating system[6]. R134a, R22, R600 are experimentally tested in a solar loop-heat-pipe façade-based heat pump water heating system[21] and R600 performed the best despite its flammability[22]. The above literature shows that the optimal filling ratio or kind of working fluid of a loop thermosyphon varies greatly according to the application conditions.

This paper aims to propose a first-of-its-kind LT-PV/T system using spiral-falling concentric copper tubes as the condenser for it is more reliable, flexible, space-saving and suitable for large-scale systems. Firstly, the prototypes of LT-PV/T systems were designed and fabricated. Then the system of this newly proposed LT structure with 3 volume-filling ratios, viz. 26.5%, 34.8%, 43.2%, of the working fluid, is experimentally tested and evaluated with 6 indexes (electrical, thermal, primary energy-saving, and exergy efficiency). After that, 3 types of the working fluid (water, ethanol and R134A), which rare research has focused on in the field of LT-PV/T, are applied in the novel LT-PV/T system and experimentally compared with the same indexes. And an additional evaluation index, a semi-empirical system efficiency model with the nominalized temperature, is also established to further access the system performance. Then the typical thermal/primary energy-saving efficiency of other LT-PV/T or LHP solar water heating systems in the published researches in recent years are listed and used to prove that the newly proposed structure has a satisfactory performance. Finally, two case studies are conducted to predict the annual performance of the LT-PV/T system in South China with the semi-empirical system efficiency models. The first case is about an individual LT-PV/T collector and the second case is about a 4 parallelly/serially combined LT-PV/T collectors system. The influence of the series/parallel mode is also compared and discussed. This comprehensive study will enable the design, optimisation and analysis of such a

new LT-PV/T system, thus promoting its wide application and achieving efficient energy performance.

2. Description of the LT-PV/T system and setups

2.1 The LT-PV/T collector

The structures of the proposed concentric copper tube heat exchanger are shown in Fig.3. It was a straight concentric copper tube at first with the inner tube of Φ12 mm and outer tube of Φ25 mm and then was spiralled into an approximating rectangular shape. After that, it was pulled into a downward spiral shape and the two outlets of the inner tube are welded to the pipes which are connected to the PV/T collector, as shown in Fig.4. A filling port, which can be used for vacuuming and liquid injection in different experiments, is inserted into the liquid returning line of each LT-PV/T collector. The evaporator consists of two collecting pipes of Φ18 mm and 7 branch pipes of Φ8 mm which are laser-welded to the back of the absorber. The absorber, an aluminium plate, is cut into 3 pieces in the direction perpendicular to the branch pipes to minimize its bend. 42 pieces of polysilicon PV cells are laminated to the aluminium absorber with TPT (Tedlar Polyester Tellar) and EVA (Ethylene Vinyl Acetate), and the package ratio is 71.5%. From the top to the bottom of the PV& absorber layer is transparent TPT, EVA, PV cells, EVA, black TPT, EVA, absorber. The glass cover, PV& absorber, evaporating pipes, insulation material (50-mm-thick polyester fibres), the backboard are assembled with a frame. The air gap between the glass cover and the absorber is 15mm.

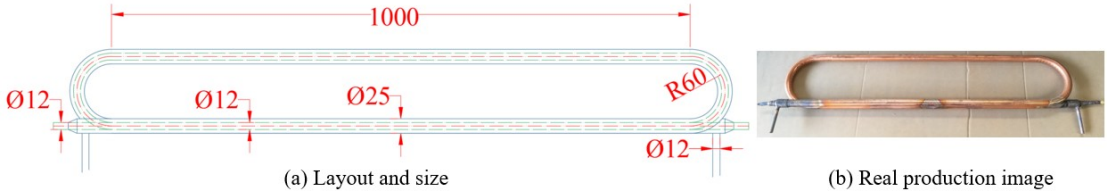

(a) Layout and size (b) Real production image

Fig. 3. The structure of the novel concentric tubes heat exchanger

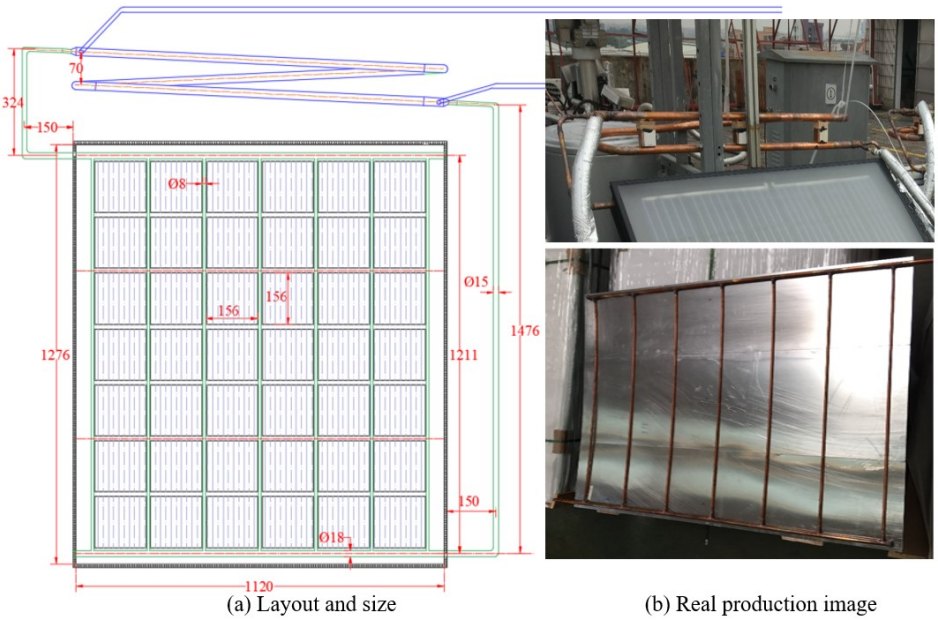

(a) Layout and size (b) Real production image

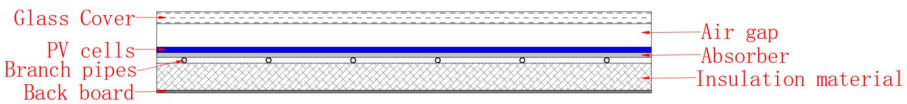

© Cross-section diagram

Fig. 4. The structure of the novel LT-PV/T

2.2 The experiment setup for investigation on filling ratio and working medium kinds

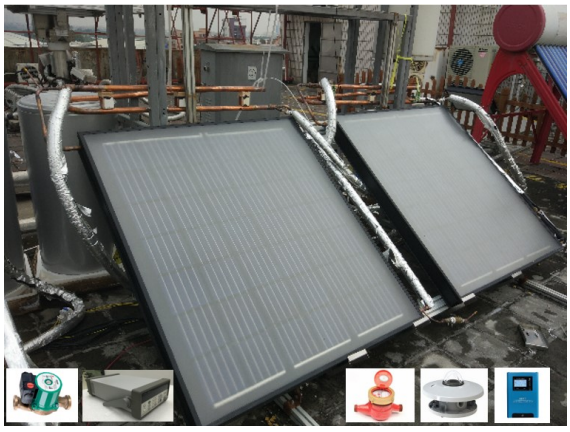

Fig. 5. The experimental setup of the novel LT-PV/T systems

The experimental setups were constructed in Dongguan, China (23°N, 113.7°E) and a series of tests were conducted according to the ISO 9806[23]. 3 identical LT-PV/T collectors were placed facing north at a 32° angle. The inner tubes of the heat exchangers are connected to the collecting pipes by copper tubes of Φ15 mm and the outer tubes are connected to the water tank of 80 L by ordinary water pipes. In the 2 groups of experiments, the loop thermosyphon pipes in the 3 LT-PV/T collectors are vacuumed at first. Then they are injected with different working fluids (water, ethanol and R134A) and then with different volume-filling ratios (26.5%, 34.8%, 43.2%) as required. All of the pipes were wrapped in insulation materials and reflective tin foils to prevent heat exchange with ambient. Cooling water was driven by water pumps of 60W and flowed at 0.14 kg/s. The MPPT was used to track the maximum power point of PV cells and store the electricity in the battery. The current signal in the circuit was transferred into a voltage signal by the Current Sensor and recorded by the data logger. T-type thermocouples and Platinum-resistance thermocouples were used to measure the temperature of the absorber and water tank. A radiometer was used to measure the solar radiation of the surface of those LT-PV/T collectors. A data logger was used to collect and record the above data. The detailed parameters are listed in Table 1.

Table 1
The parameters of the sensor/instruments.

Sensor/Instrument	Type	Full Scale	Accuracy
Radiometer	TBQ-2	0 -2000 W/m^2	±2%
Flowmeter	LXSR	0.03 -3 m^3/h	±3%
Thermocouple	T	-250 – 350 ℃	±0.2℃
Platinum-resistance Thermocouple	Pt100	-50 -300 ℃	±0.15 ℃
MPPT	JieCheng 24V	18 -150 V	±1.5%
Current Sensor	HK-D41	0 -10 A	±1.5%
Data logger	Agilent 34970		

2.3 The simulation setup for the case study of 4 parallelly/serially-combined LT-PV/T collectors system

Since one of the great advantages of the proposed LT-PV/T lies in its simple and flexible connection between concentric copper tube heat exchangers when using several LT-PV/T collectors in combination as introduced above, the combination using is tried and the performance is predicted. 4 LT-PV/T collectors are designed to be combined in series and parallel, as presented by Fig. 6:

(1) For both combination methods, the water tank is fourfold 80 L and the water flows at 0.14 kg/s, in which case the semi-empirical system efficiency models make sense.

(2) In the parallel connection, water flows out the water tank and separately flows into each heat exchanger and then finally back together to the water tank.

(3) In the series connection, water flows out the water tank and through 4 heat exchangers one by one and then flows back to the water tank.

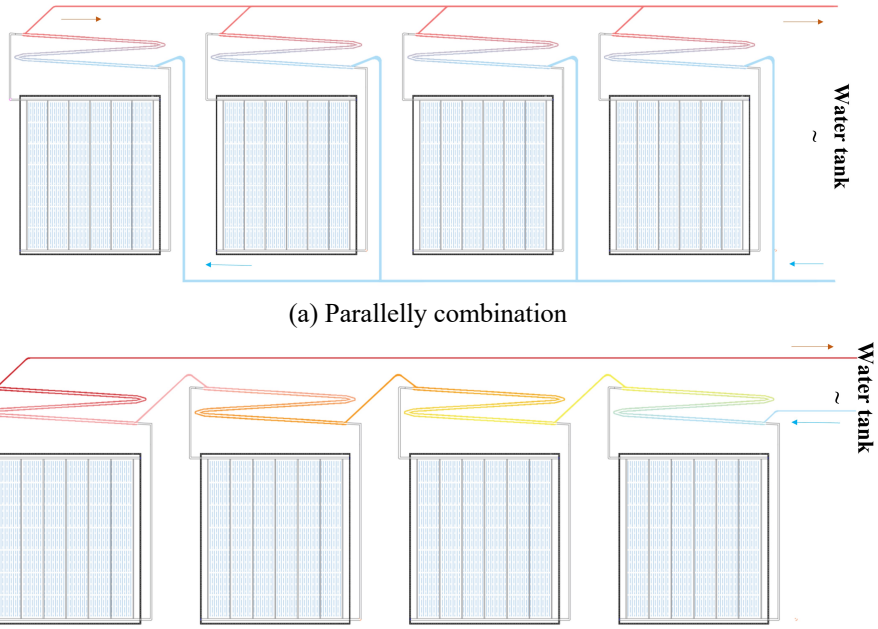

(a) Parallelly combination

(b) Serially combination

Fig. 6. The simulation setup for 4 serially/parallelly-combined LT-PV/T collectors system

3. Methodology

3.1 Performance evaluation index

The instantaneous electrical efficiency and the thermal efficiency with 5-minutes-interval of the LT-PV/T system is calculated as[24]:

$$\eta_{\mathrm{pv}} = \frac{\int_t^{t+\Delta t} E_{pv}\,dt}{\int_t^{t+\Delta t} G\ \mathrm{d}t \times A_{PV}} \tag{1}$$

$$\eta_{th} = \frac{m_{water} \times C_{water} \times \Delta T_{\tan k}}{\int_t^{t+\Delta t} G\,dt \times A_b} \tag{2}$$

The overall energy efficiency and the primary energy-saving efficiency is calculated as:

$$\eta_{overall} = \eta_{th} + \zeta \cdot \eta_{\mathrm{pv}} \tag{3}$$

$$\eta_f = \eta_{th} + \frac{\eta_{pv}\zeta}{\xi} \tag{4}$$

$$\zeta = \frac{A_{PV}}{A_b} \tag{5}$$

Based on the semi-empirical system efficiency model that Huang and Du proposed [25], with a variable ($\frac{T_i - \overline{T_a}}{H_t}$) to evaluate the thermal performance, a general equation for solar thermal efficiency can be derived, and the linear correlation between the thermal efficiency every 5 minutes and the

normalized temperature ($\frac{T_i-\overline{T_a}}{H_t}$)is built to evaluate the thermal performance considering the dynamic initial water tank temperature, solar radiation and average ambient temperature, as[26, 27]:

$$\eta_{th}=\eta_{th}^{*}-U_1\frac{T_i-\overline{T_a}}{H_t} \tag{6}$$

where η_{th}^{*} is the typical thermal efficiency in condition that the initial water tank temperature equals the ambient temperature, while U_1 is thermal heat loss coefficient (KJ/m^{2}K).

Correspondingly, the primary energy-saving efficiency is expressed by:

$$\eta_f=\eta_f^{*}-U_2\frac{T_i-\overline{T_a}}{H_t} \tag{7}$$

where η_f^{*} and U_2 is the typical primary energy-saving efficiency and primary energy loss coefficient (KJ/m^2·K) respectively;

Exergy is defined as the amount of work a system can perform when it is brought into thermodynamic equilibrium with its environment. Exergy efficiency, also known as second-law efficiency, is used to calculate the effectiveness of the LT-PV/T system, expressing how much of the work capacity we can utilize. The exergy efficiency of the thermal heat gain, the electrical output is calculated by:

$$\varepsilon_{th}=\frac{\sum \dot{Ex}_{th}}{\sum Ex_{sun}A_b} \tag{8}$$

$$\varepsilon_{pv}=\frac{\sum \dot{Ex}_{pv}}{\sum Ex_{sun}A_b} \tag{9}$$

where the thermal exergy output, the electrical exergy output and the solar exergy input are calculated by[26, 28]:

$$\dot{Ex}_{pv}=E_{pv} \tag{10}$$

$$\dot{Ex}_{th}=Q\left(1-\frac{T_a}{T_2}\right) \tag{11}$$

$$\dot{Ex}_{sun}=G\left(1-\frac{4}{3}\left(\frac{T_a}{T_{sun}}\right)-\frac{1}{3}\left(\frac{T_a}{T_{sun}}\right)^4\right) \tag{12}$$

where T_2 is the final water tank temperature (K).

The overall exergy efficiency is expressed as:

$$\varepsilon_{overall}=\varepsilon_{th}+\varepsilon_{\mathrm{pv}} \tag{13}$$

Since the energy efficiency and exergy efficiency are indirectly measured, the uncertainty can be calculated as:

$$y=f(x_1,x_2,.....,x_n) \tag{14}$$

$$\frac{\Delta y}{y}=\left[\left(\frac{\partial f}{\partial x_1}\right)^2\left(\frac{\Delta x_1}{y}\right)^2+\left(\frac{\partial f}{\partial x_2}\right)^2\left(\frac{\Delta x_2}{y}\right)^2+.....+\left(\frac{\partial f}{\partial x_n}\right)^2\left(\frac{\Delta x_n}{y}\right)^2\right]^{1/2} \tag{15}$$

3.2 Solution methodology for the case study of annual performance

3.2.1 An individual LT-PV/T collector

The semi-empirical system efficiency models are used in the prediction of annual performance. The interval is also set as 5 minutes. The algorithm used for calculating is indicated by a flow chart in Fig.7, detailed as follows:

(1)Input the weather data like the solar radiation, ambient temperature, the underground water temperature of each hour of a whole year. Input the time step. Input the semi-empirical models about typical thermal efficiency and typical primary energy-saving efficiency.

(2) Enter the date loop. In each loop, the performance of a whole day is calculated.

(3) In a date loop, the underground water is taken as the initial water tank temperature. Then enter the time loop. In each time loop, the performance of one timestep is calculated.

(4) In each time loop, the solar radiation and ambient temperature are read at first. It is assumed that the LHP will start running if solar radiation is larger than 100W/m^2 because the equivalent thermal resistance of the loop thermosyphon will increase when the heat flux is very low. The thermal and primary efficiency are calculated. If the thermal efficiency is larger than 0, the heat gain and primary energy gain is calculated. It is assumed the loop thermosyphon will stop work and will not release heat if the calculated thermal efficiency is smaller than 0, considering the thermal-diode[29] characteristic of loop thermosyphon in LT-PV/T.

(5) The system generates electricity as long as the solar radiation on the PV surface is larger than 0. The electricity efficiency is calculated by the primary energy-saving efficiency and the thermal efficiency of this time step.

(6) The water temperature increase is calculated by the heat gain calculated in one timestep and then the initial water temperature of the next time step is calculated.

(7) In a day loop, the energy output of each time step are summed up as the daily performance after all the time loops are finished.

(8) Output the heat gain, electricity yield, primary energy gain of each day of a year.

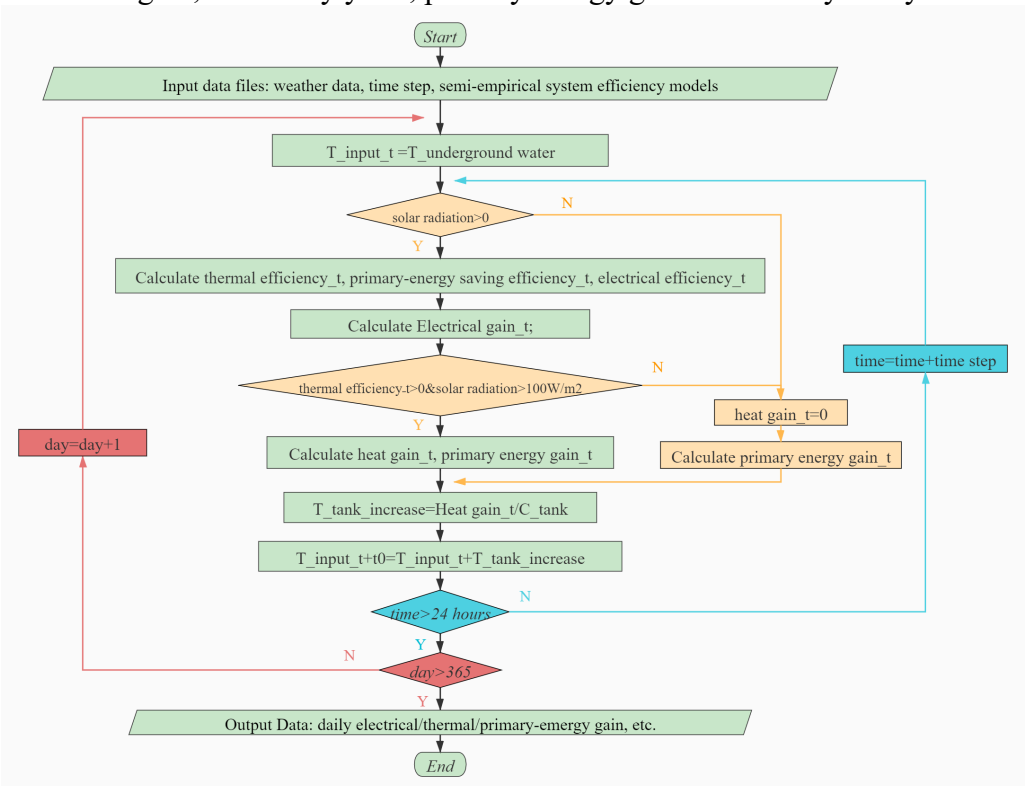

Fig. 7. Flow chart for annual performance prediction of an individual LT-PV/T collector

3.2.2 The 4 parallelly/serially-combined LT-PV/T collectors system

For the parallelly-combined or serially-combined LT-PV/T collectors system, the algorithm used is slightly different.

(1) The calculation of parallelly-combined LT-PV/T collectors system is similar to an individual collector system, as shown in Fig.7. the inlet water temperature of each collector is taken as the water tank temperature, while the outlet hot water contributes together to the heating of water tank.

(2) For the serially combined LT-PV/T collectors system, the outlet water temperature of the former exchanger is also the inlet temperature of the next one. The algorithm used for calculating is indicated by a flow chart in Fig.8.

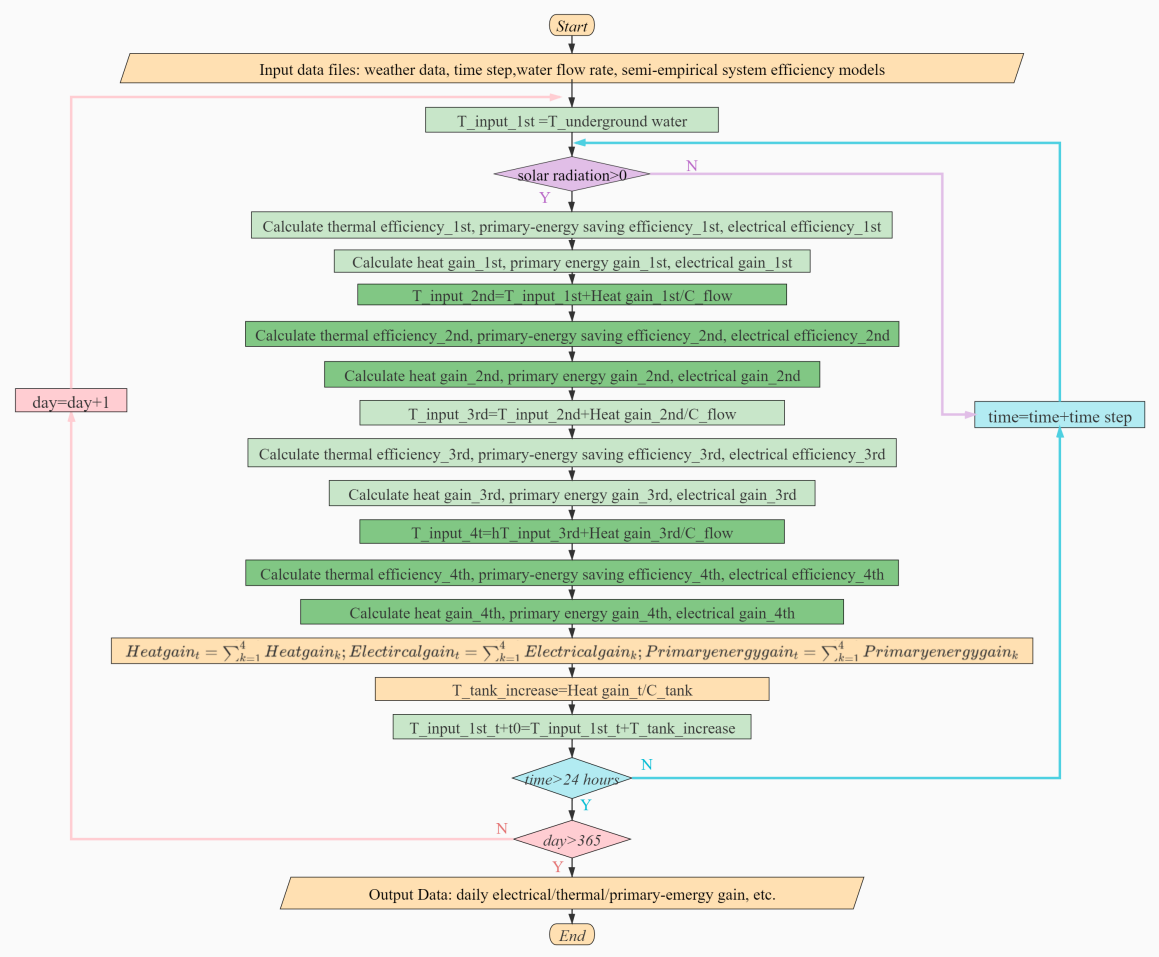

Fig. 8. Flow chart for annual performance prediction of 4 LT-PV/T collectors in series

4. Results and Discussion

4.1 Filling ratio

Firstly, the LT-PV/T systems with 3 filling ratios of water as the working fluid were experimentally tested, and the performance is compared to explore the proper ratio. The weather conditions are drawn in Fig.9.

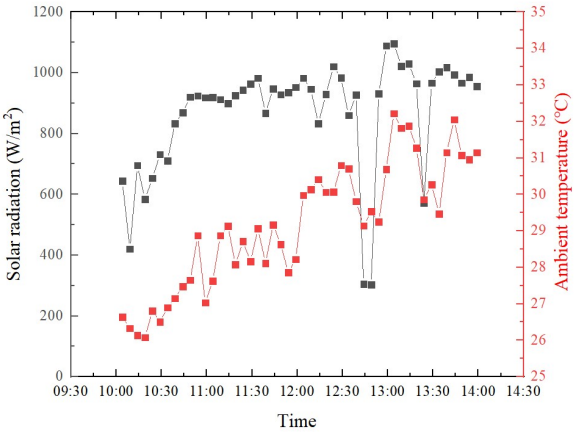

Fig. 9. Weather conditions

Table 2 gives the results of the all-day electrical, thermal, overall, primary energy-saving and exergy efficiency. Fig.10 shows the instantaneous thermal efficiency with 5-minutes-interval. Throughout the whole day, LT-PV/T of 34.8% filling ratio (hereinafter referred to as LT-PV/T-34.8%) shows the best heat transfer performance and thus the best thermal efficiency among the three systems, a little higher than the LT-PV/T of 43.2% filling ratio (hereinafter referred to as LT-PV/T-43.2%). The thermal efficiency of the LT-PV/T of 26.5% filling ratio (hereinafter referred to as LT-PV/T-26.5%) is nearly 24% relatively lower than that of the other two systems, which indicates that it has a weaker heat transfer function. It would not have enough working fluid, so when the solar irradiation is strong, only part of the irradiation can be absorbed into the latent heat of the working fluid. The amount of working fluid limits the total amount of solar irradiation that can be absorbed and thus the heat transfer capacity. What's more, another reason lies in the thermal loss and thermal resistance. A low filling ratio also means that the evaporative liquid surface level is low, that is, the system's thermal resistance becomes greater. Moreover, the steam evaporated rises along the pipes, keeping absorbing heat and quickly heats up due to its relatively small thermal capacity, and therefore higher temperature makes the heat loss of the system larger.

Table 2
The LHPs with 3 filling ratio.

	A	B	C
Volume-filling ratio	26.5%	34.8%	43.2%
Electrical efficiency	7.23%	8.47%	7.91%
Thermal efficiency	27.35%	36.78%	35.96%
Overall efficiency	32.52%	42.83%	41.62%
Primary energy-saving efficiency	40.94%	52.71%	50.85%
Exergy efficiency	5.86%	7.30%	6.74%

But for the LT-PV/T-43.2%, the reason for its relatively a little bit lower performance lies in the opposite. A higher filling ratio means higher thermal capacity and higher liquid level of the working fluid. The gas bubbles or heated fluid at the lower position in evaporating section rise more slowly due to the pressure of the liquid, thus causing a relatively slower heat transfer rate, though not quite obvious.

The cooling performance directly influences the temperature of the solar cells, as shown in Fig.11. As time goes on, the PV temperature of the three systems rises steadily and the electrical efficiency shows a downward trend. The PV temperature of the LT-PV/T-26.5% is higher than that of the other two systems, and therefore the all-day electrical efficiency is 14.6% relatively lower than the LT-PV/T-34.8%, while that of the LT-PV/T-43.2% system is 6.7% relatively lower than the LT-PV/T-34.8% system.

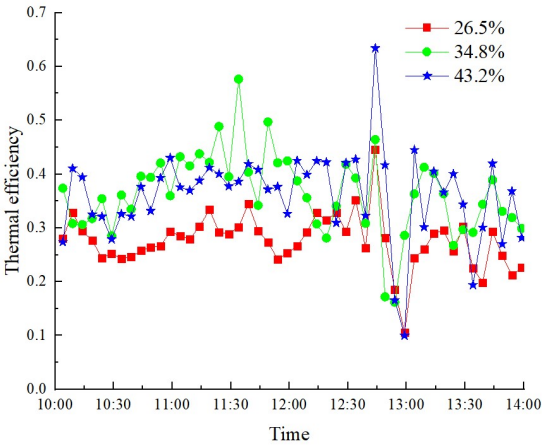

Fig. 10. Instantaneous thermal efficiency

Fig.11 shows that the LT-PV/T-34.8% has a slightly higher electrical efficiency than the LT-PV/T-43.2% system because of the relatively lower PV temperature, but their gap is not as large as their comparison to the LT-PV/T-26.5%. Meanwhile, for the LT-PV/T-34.8% and the LT-PV/T-43.2%, their daily thermal performance, overall efficiency and primary energy-saving efficiency are shown to be similar with a very small difference. The exergy efficiency of each LT-PV/T system varies greatly. Fig.12 shows the electrical exergy efficiency, thermal exergy efficiency as well as overall exergy efficiency of the three LT-PV/T systems. Since the quality of the electricity is quite higher than the thermal energy, the electrical exergy plays a more important role in the overall exergy efficiency and therefore their fluctuations show to be similar, notwithstanding the slowly rising thermal exergy efficiency because of the climbing operating temperature. The overall exergy efficiency of the LT-PV/T-34.8% is 24.6% relatively higher than the LT-PV/T-26.5%, and the LT-PV/T-43.2% is 15.0% relatively higher than the latter.

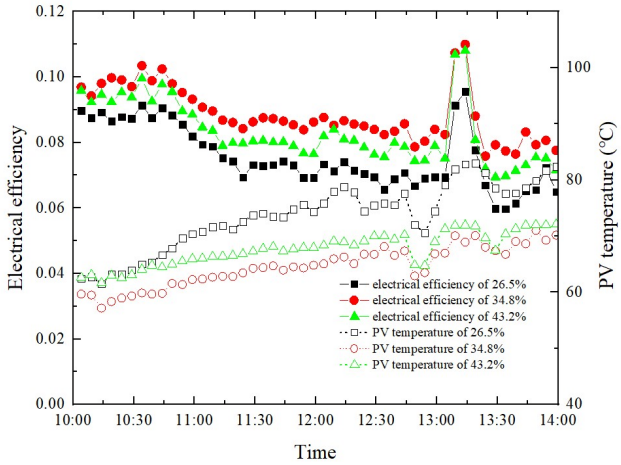

Fig. 11. PV temperature and electrical performance

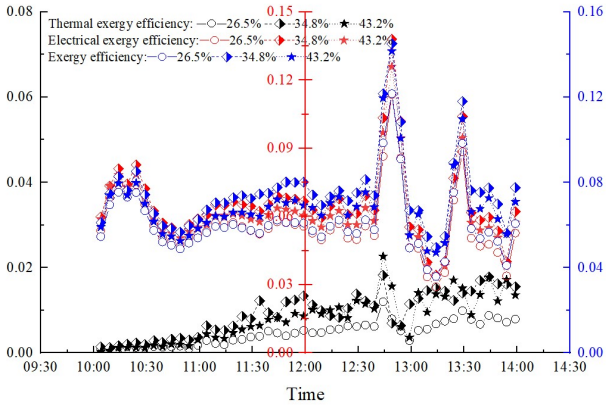

Fig. 12. Exergy efficiency

4.2. Working fluid

Then the performance of three loop-pipe PV/T systems with three kinds of the typical working fluid, viz. water, ethanol, and R134a, is experimentally compared and discussed. The filling ratio of each system is roughly set as 40%, as listed in Table 3. The weather conditions are drawn in Fig.13.

Table 3
The LHPs with 3 kinds of the working fluid

Working fluid	Mass	Volume-filling ratio
	g	%
water	740	43.3
Ethanol	540	40.0
R134a	860	41.6

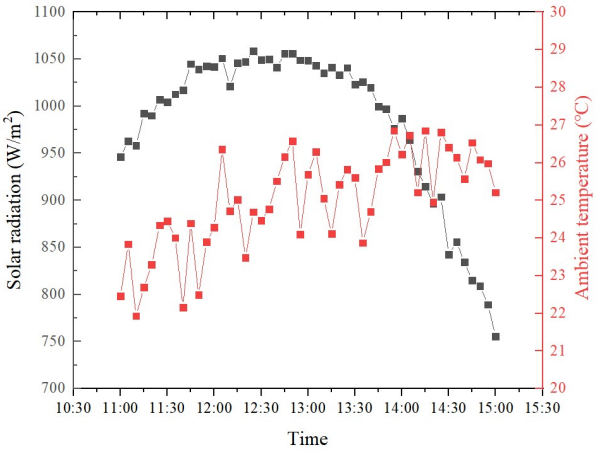

Fig. 13. Weather conditions

The all-day electrical and thermal performance of the 3 LT-PV/Ts are summarized and listed in Table 4 and the uncertainty are listed in Table 6. Among the 3 systems, the LT-PV/T with ethanol and R134a perform better than the LT-PV/T with water. In particular, the LT-PV/T with R134a shows the best heat transfer effect and thus the lowest solar cells temperature, the highest electrical efficiency and thermal efficiency. The solar cells temperature of LT-PV/T with R134a is nearly 40 ℃ lower than that of the LT-PV/T with water at 11:00, as illustrated in Fig.14. As time goes on, the PV temperature climbs gradually because of the increasing solar radiation and water tank temperature, and the temperature difference between the 3 systems are narrowed down to 10-20 ℃. The fluctuations in electrical efficiency correspond to PV temperature. The highest electrical efficiency of the three systems is 7.69%, 8.41%, 9.31% respectively, achieved at the beginning of the experiment.

Table 4
The all-day performance of three loop-pipe PV/T systems with different working fluids.

Working fluid	Water	Ethanol	R134a
Electrical efficiency	7.49%	7.70%	8.29%
Thermal efficiency	26.20%	30.29%	37.46%
Overall efficiency	31.55%	35.80%	43.38%
Primary energy-saving efficiency	40.29%	44.79%	53.05%
Exergy efficiency	6.30%	7.20%	8.30%

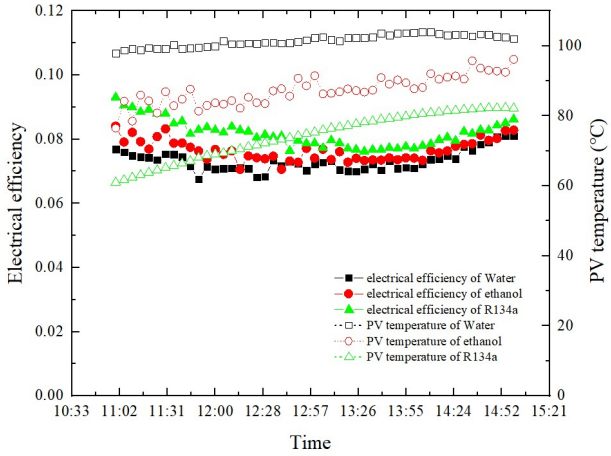

Fig. 14. PV temperature and electrical performance

As mentioned above, the working fluid transfers the thermal from the absorbing plate to the water relying on the evaporating, condensing, and cycling inside the loop thermosyphons, so the instantaneous thermal efficiency of the three systems also shows a slight climb in the early stage of the experiment as shown in Fig.15 due to the increased heat gain and temperature difference. And then the thermal efficiency declines gradually due to the climbing water tank temperature. The all-day thermal efficiency of the LT-PV/T with water is 11.3% lower than the R134a and 4.1% lower than the ethanol.

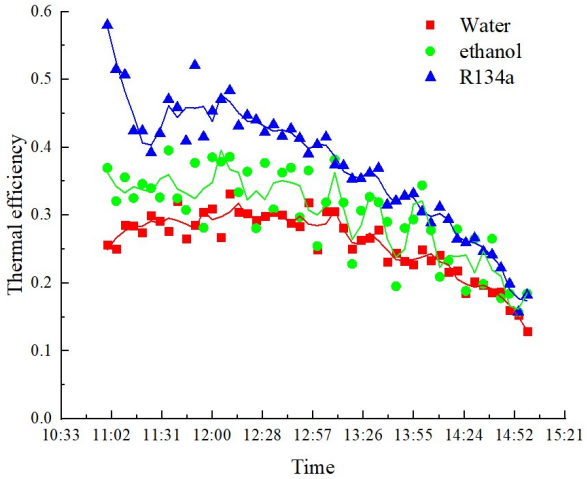

Fig. 15. Instantaneous thermal efficiency

The linear correlations between the thermal efficiency with the normalized temperature are calculated, as shown in Fig.16. The typical thermal efficiency when the incoming water temperature is equal to the ambient temperature is 33.1%, 43.2% and 57.8% respectively for the water, ethanol and R134a. The heat loss coefficient is -2.63 KJ/m^2, -2.70 KJ/m^2, and –3.42 KJ/m^2 respectively. With the increase of solar intensity and the ambient temperature and the decreasing of initial water temperature, the thermal efficiency increased accordingly, while the impact on the LT-PV/T-water is the lowest.

$$\eta_{th,water} = 0.331 - 2.63 \cdot \frac{T_i - \overline{T_a}}{H_t} \quad (15)$$

$$\eta_{th,ethanol} = 0.432 - 2.70 \cdot \frac{T_i - \overline{T_a}}{H_t} \quad (16)$$

$$\eta_{th,R134a} = 0.578 - 3.42 \cdot \frac{T_i - \overline{T_a}}{H_t} \quad (17)$$

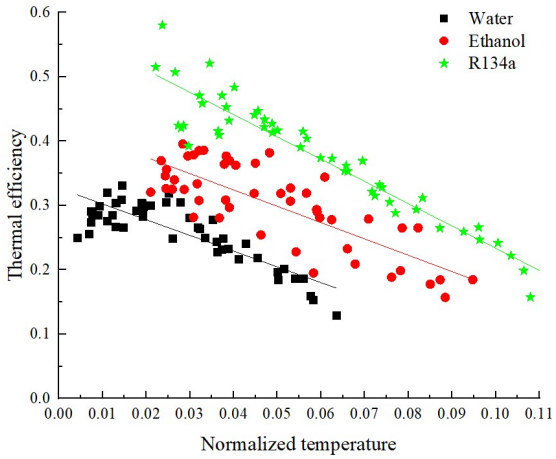

Fig. 16. Linear correlations between the thermal efficiency with the normalized temperature

Similarly, the typical primary energy-saving efficiency of the three systems is 47.0%, 58.6% and 74.0% respectively, as shown in Fig.17.

$$\eta_{f,water} = 0.470 - 2.79 \cdot \frac{T_i - \overline{T_a}}{H_t} \quad (18)$$

$$\eta_{f,ethanol} = 0.586 - 2.95 \cdot \frac{T_i - \overline{T_a}}{H_t} \quad (19)$$

$$\eta_{f,R134a} = 0.740 - 3.64 \cdot \frac{T_i - \overline{T_a}}{H_t} \quad (20)$$

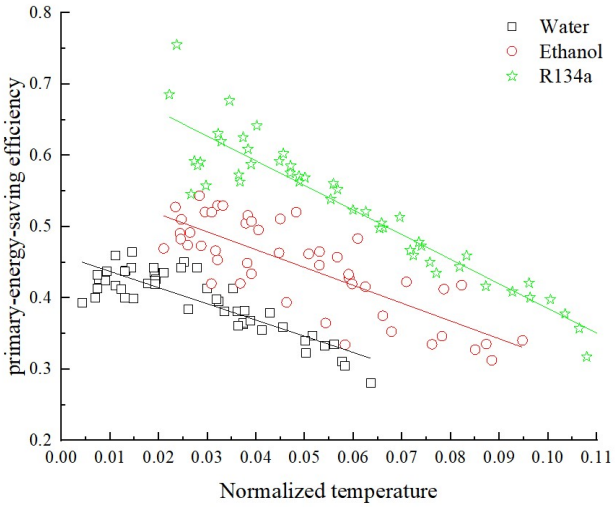

Fig. 17. Linear correlations between the primary energy-saving efficiency with the normalized temperature

Table 5 listed the typical thermal/primary energy-saving efficiency of the published LT-PV/T or LHP solar water heating systems, it indicates that the proposed LT-PV/T in this paper, especially with R134a as working fluid, performs well with obvious advantages.

Table 5
The typical efficiency of the published researches about LT-PV/T or LT/LHP solar water heating systems

System	Working fluid	Packing factor	Performance
MC-LHP-PV/T[7]	R134a	86%	Typical thermal efficiency: $\eta_{th}^{*}=0.519-8.8(T_i-\overline{T_a})/G$
LT-PV/T[12]	R600a	50%	Typical primary energy-saving efficiency: $\eta_{f}^{*}=0.42-12.9(T_i-\overline{T_a})/G$
PV/LHP/solar assisted heat pump water heating system[13]	R22	53%	Daily thermal efficiency in transition seasons, summer and winter: 53.64%, 52.63% and 47.84%
Pump-forced wickless LT-SWH system[30]	R600a	0	Typical thermal efficiency: $\eta_{th}^{*}=0.514-0.138(T_i-\overline{T_a})/G$
LT-solar collector[12]	R600a	0	Typical thermal efficiency: $\eta_{th}^{*}=0.58-7.57(T_i-\overline{T_a})/G$

The thermal, electrical and overall exergy efficiency is calculated and presented in Fig.18. The thermal exergy efficiency of all three systems is concave down, and the highest figure is 1.08%, 2.02% and 2.71% respectively, achieved at the middle time because of the high water temperature. Inversely, though the electrical exergy output of the three systems is also the highest in the middle day, the solar exergy input is also the highest, therefore, the electrical exergy efficiency shows to be concave up during the whole day. The electrical exergy accounts for the main part of the overall exergy efficiency because of its high quality. Taking the thermal exergy, electrical exergy and the solar cell packing factor into account, the overall exergy efficiency of the LT-PV/T with water and ethanol rises gradually throughout the whole day, while the LT-PV/T with R134a shows to be a parabola slightly opening down. The highest overall exergy efficiency of the three systems is 6.89%, 6.98% and 8.04% respectively.

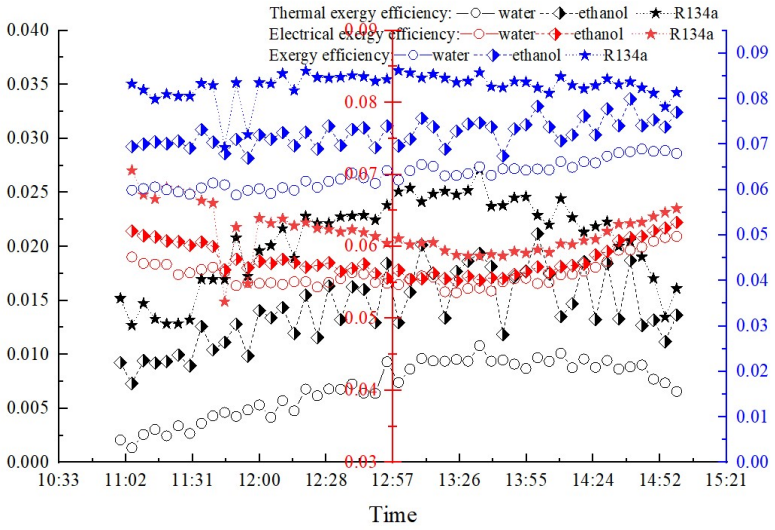

Fig. 18. Exergy efficiency

Table 6
The uncertainty of the indirectly measured data.

	Group 1: Volume-filling ratio			Group 2: Working fluid types		
	26.5%	34.8%	43.2%	Water	Ethanol	R134a
Electrical efficiency	0.07%	0.07%	0.07%	0.07%	0.07%	0.07%
Thermal efficiency	1.97%	1.40%	1.44%	1.80%	1.55%	1.25%
Overall efficiency	1.56%	1.15%	1.12%	1.40%	1.24%	1.03%
Primary energy-saving efficiency	1.32%	1.00%	1.03%	1.17%	1.05%	0.89%
Exergy efficiency	0.95%	1.02%	1.25%	1.23%	1.76%	1.84%

4.3 Case of annual performance prediction of an individual LT-PV/T collector system

Based on the experimental results above, LT-PV/T with R134a shows a satisfactory performance on the typical autumn day. It is also meaningful to bring in the other season weather conditions to explore its annual performances for the application. Therefore, the hourly weather data of Hefei, a city in South China with four distinctive seasons, are brought in from Energy Plus, and the key parameters are plotted in Fig.19. It is based on the real data in the area measured over the past few years, so the daily solar radiation shows a significant fluctuation with days going on due to the weather like rain, snow and cloudy, besides the earth revolution.

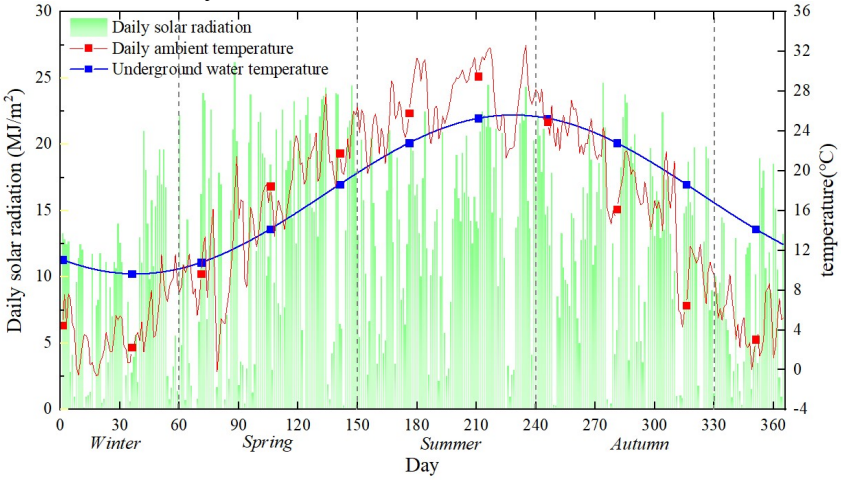

Fig. 19. Annual environment condition

The predicted annual performances are presented monthly in Fig.20, and the seasonal performances are summarized in Table 7. The variation trends of the energy gains are influenced simultaneity by the daily solar radiation, ambient and underground water temperature. From the perspective of season, the Summer performs the highest thermal and electricity yield of 602.8 MJ and 98.1 MJ respectively due to the higher solar radiation and ambient temperature, though with the relatively warmer underground water. Followed is the Spring, with a heat gain of 557.1 MJ and electricity gain of 91.2 MJ. No doubt that winter has the lowest thermal yield and lowest electricity yield which is 47% and 58% of the Summer due to the low radiation and cold ambient. An interesting thing is that though the overall performance in Summer is higher than Spring when talking about monthly output, the fluctuation is not an “n” but an “M” shape. A dip appears in June and July because of the plum rain season coming. It also shows that the performance climbing from March to May is the quickest than that from June to August, caused by the highly increasing ambient temperature. The highest thermal is obtained in May and highest electricity output is achieved in August.

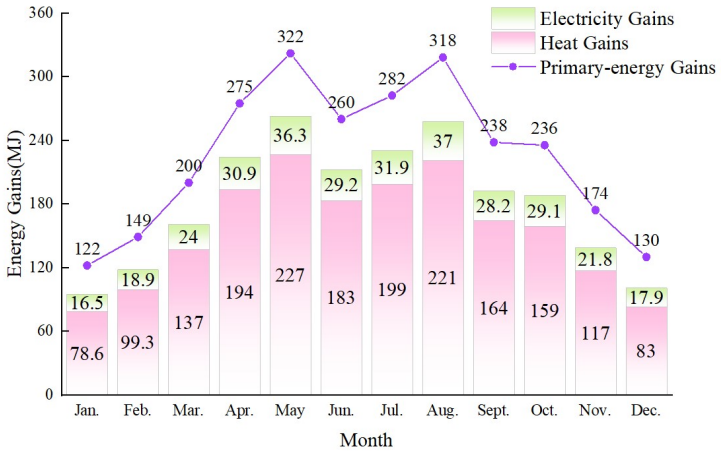

Fig. 20. Monthly performance

Table 7
The seasonal performance prediction of the novel LT-PV/T system.

	Solar radiation	Heat gains	Electrical gains	Primary energy gains
	MJ/m^2	MJ	MJ	MJ
Spring	1186.5	557.1	91.2	797.2
Summer	1274.2	602.8	98.1	860.9
Autumn	1072.3	440.2	79.1	648.2
Winter	768.4	260.9	53.3	401.3

4.4 Case study of the annual performance of 4 serially/parallelly-combined LT-PV/T collectors system

The predicted monthly performance of the combination utilization in parallel and series are illustrated and compared in Fig.21, and the yearly performance comparison is listed in Table 8. The monthly fluctuations of the summary of the thermal and primary energy gains show to be similar between the series connection and parallel connection. For the four LHP-PVT collectors in series connection, they show a gradual decrease in thermal output and primary energy output because of the increasing input cooling water temperature and therefore the decreasing thermal and primary energy-saving efficiency. Therefore, the whole-year heat gain of the parallel system is 2.28% higher than the series system, which is not too much. The slightly lower thermal performance, which means the slightly slower water temperature increase, causes the lower input water temperature of the first LT-PV/T collector in the series connection and therefore the higher thermal performance than the collector in the parallel connection. But the temperature difference, both among the 4 collectors in the series connection and among the two connection methods, is too small to show a difference in electrical output. The whole-year primary energy gain of the series system is 1.60% higher than the parallel connection.

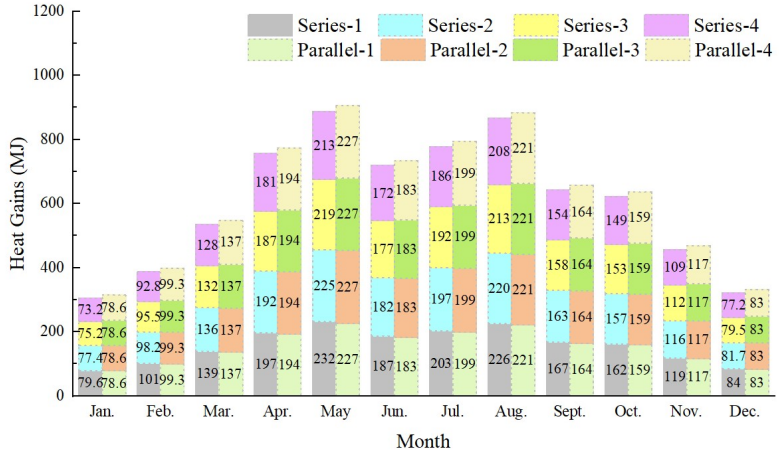

(a) Heat Gains

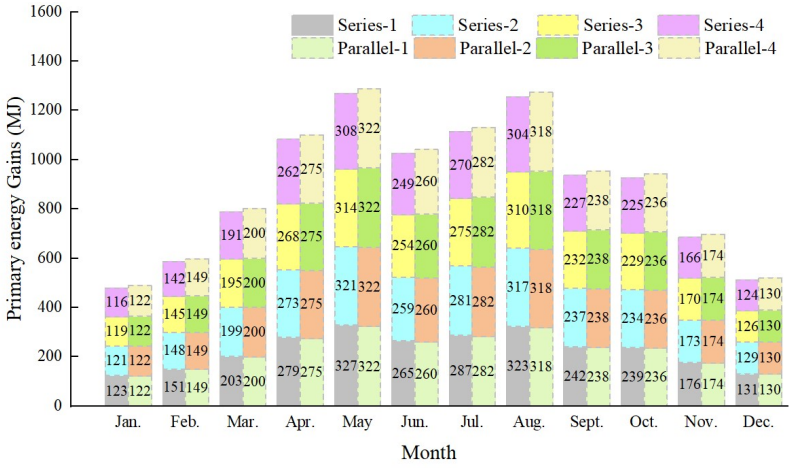

(b) Primary energy gains

Fig. 21. Monthly performance prediction of 4 serially/parallelly-combined LT-PV/T collectors system

Table 8

The annual performance prediction of 4 serially/parallelly-combined LT-PV/T collectors system

Energy Gains (MJ)	In parallel			In series		
	Sum	Each		Sum	Each	
Heat	7443.8	N1:	1861.0	7277.9	N1:	1896.9
		N2:	1861.0		N2:	1844.3
		N3:	1861.0		N3:	1793.2
		N4:	1861.0		N4:	1743. 5
Electricity	1286.9	N1:	321.7	1285.0	N1:	323.1
		N2:	321.7		N2:	321.9
		N3:	321.7		N3:	320.7
		N4:	321.7		N4:	319.4
Primary energy	10830.3	N1:	2707.6	10659.5	N1:	2747.3
		N2:	2707.6		N2:	2691.3
		N3:	2707.6		N3:	2636.9
		N4:	2707.6		N4:	2584.0

5. Conclusions

The condensers of LHP-hot water heating/PV/T/heat pump systems are usually integrated inside water tanks, in which case some challenges may arise when the adiabatic section of the heat pipes of several LT-PV/T collectors are connected for combination utilization. So this research proposed a novel LT-PV/T using a concentric copper tube heat exchanger with a rectangular spiral

descent as the condenser, which is connected to an evaporator beneath the absorber. The inner tube acts as the condensing section for the gaseous working fluid and the cooling water flows in the outer tube in the opposite direction of the working fluid. The system is first-of-its-kind and has obvious advantages in a variety of areas. Its structure offers advantages to its reliability, flexibility, space-saving and suitability for large-scale applications. This paper introduced the conception and early-stage research of this newly proposed structure, which will enable design, optimisation and analysis of such a new LT-PV/T system, thus promoting its wide application and achieving efficient energy performance.

The performance of LT-PV/T with different filling ratios (26.5%, 34.8% and 43.2%) is experimentally explored at first. Judging from the first law of thermodynamics, the LT-PV/T-34.8% and LT-PV/T-43.2% perform similarly in thermal, overall, and primary energy-saving efficiency though the former one shows higher electricity output. The heat transferring and cooling function of the LT-PV/T-26.5% is weaker than the other two systems, thus leading to the lowest electrical, thermal, overall and primary energy-saving efficiency. Judging from the second law of thermodynamics, considering the high quality of electricity, the LT-PV/T-34.8% has the highest exergy efficiency of 7.30%.

Then the performance of LT-PV/T with different working fluids (water, ethanol and R134A) is experimentally studied. The LT-PV/T with R134a as the working fluid with the filling ratio of about 40% performs significantly better than the ethanol, then better than the water in regards to both the first and second law of thermodynamics. The typical thermal efficiency is 32.7%, 42.6% and 58.0% respectively for the water, ethanol and R134a LT-PV/T systems, while the typical primary energy-saving efficiency of the three systems is 46.0%, 56.8% and 73.0% respectively. Compared to the published LT-PV/T or LHP solar water heating systems, the newly proposed LT-PV/T in this paper, especially with R134a as the working fluid, performs well with obvious advantages.

Two case studies in South China (an individual collector & a 4 parallelly/serially-combined LT-PV/T collectors system) are conducted with the semi-empirical models. For the predicted annual performances of an individual LT-PV/T collector system with R134a, the Summer performs the highest thermal and electricity yield of 602.8 MJ and 98.1 MJ respectively due to the higher solar radiation and ambient temperature, followed by the Spring with heat gain of 557.1 MJ and electricity gain of 91.2 MJ. The fluctuation of the monthly prediction is not an “n” but an “M” shape because of the plum rain season in June and July. The highest thermal is obtained in May and highest electricity output is achieved in August.

For the combination utilization of 4 LHP/PV/T, the annual heat gain and primary energy gain of the parallel system is 2.28% and 1.60% respectively higher than that of the series system, though not too much. So it barely influences the electricity output because the temperature difference is quite small. Therefore, though the parallel connection performs better, one can choose whichever connection method according to the actual situation on the roof or façade of the building.

The potential of this system lies not only in its superior performance but also in the ease and reliability of combined applications. The next step of the research of this new LT-PV/T system is to build mathematical models for the more refined optimization of the structure for both the concentric copper tube heat exchanger and the evaporator, as well as the combination utilization method.

Acknowledgement

This work has been supported financially by the national science foundation of China (No. 51878636) and the China scholarship council (No.202006340111), which is gratefully acknowledged by the authors.

Reference

[1] M.A. Green, E.D. Dunlop, J. Hohl- Ebinger, M. Yoshita, N. Kopidakis, X. Hao, Solar cell efficiency tables (Version 58), Progress in Photovoltaics: Research and Applications 29(7) (2021) 657-667.
[2] T.T. Chow, A review on photovoltaic/thermal hybrid solar technology, Applied Energy 87(2) (2010) 365-379.
[3] Z. Li, J. Ji, W. Yuan, Z. Song, X. Ren, M.M. Uddin, K. Luo, X. Zhao, Experimental and numerical investigations on the performance of a G-PV/T system comparing with A-PV/T system, Energy 194 (2020).
[4] T. Zhang, W. Zheng, L. Wang, Z. Yan, M. Hu, Experimental study and numerical validation on the effect of inclination angle to the thermal performance of solar heat pipe photovoltaic/thermal system, Energy 223 (2021).
[5] M. Modjinou, J. Ji, W.Q. Yuan, F. Zhou, S. Holliday, A. Waqas, X.D. Zhao, Performance comparison of encapsulated PCM PV/T, microchannel heat pipe PV/T and conventional PV/T systems, Energy 166 (2019) 1249-1266.
[6] X. Zhao, Z. Wang, Q. Tang, Theoretical investigation of the performance of a novel loop heat pipe solar water heating system for use in Beijing, China, Applied Thermal Engineering 30(16) (2010) 2526-2536.
[7] M. Yu, F. Chen, S. Zheng, J. Zhou, X. Zhao, Z. Wang, G. Li, J. Li, Y. Fan, J. Ji, T.M.O. Diallo, D. Hardy, Experimental Investigation of a Novel Solar Micro-Channel Loop-Heat-Pipe Photovoltaic/Thermal (MC-LHP-PV/T) System for Heat and Power Generation, Applied Energy 256 (2019).
[8] H. Li, Y. Sun, Performance optimization and benefit analyses of a photovoltaic loop heat pipe/solar assisted heat pump water heating system, Renewable Energy 134 (2019) 1240-1247.
[9] Y. Cui, J. Zhu, S. Zoras, J. Zhang, Comprehensive review of the recent advances in PV/T system with loop-pipe configuration and nanofluid, Renewable and Sustainable Energy Reviews 135 (2021).
[10] X. Ren, M. Yu, X. Zhao, J. Li, S. Zheng, F. Chen, Z. Wang, J. Zhou, G. Pei, J. Ji, Assessment of the cost reduction potential of a novel loop-heat-pipe solar photovoltaic/thermal system by employing the distributed parameter model, Energy (2019).
[11] X. Zhang, X. Zhao, J. Shen, X. Hu, X. Liu, J. Xu, Design, fabrication and experimental study of a solar photovoltaic/loop-heat-pipe based heat pump system, Solar Energy 97 (2013) 551-568.
[12] T. Zhang, Z. Yan, G. Pei, Q. Zhu, J. Ji, Experimental optimization on the volume-filling ratio of a loop thermosyphon photovoltaic/thermal system, Renewable Energy 143 (2019) 233-242.
[13] H. Li, Y. Sun, Operational performance study on a photovoltaic loop heat pipe/solar assisted heat pump water heating system, Energy and Buildings 158 (2018) 861-872.
[14] T.M.O. Diallo, M. Yu, J. Zhou, X. Zhao, S. Shittu, G. Li, J. Ji, D. Hardy, Energy performance analysis of a novel solar PVT loop heat pipe employing a microchannel heat pipe evaporator and a PCM triple heat exchanger, Energy 167 (2019) 866-888.
[15] Y. Liu, Z. Li, Y. Li, Y. Jiang, D. Tang, Heat transfer and instability characteristics of a loop thermosyphon with wide range of filling ratios, Applied Thermal Engineering 151 (2019) 262-271.
[16] Y. Liu, Z. Li, Y. Li, S. Kim, Y. Jiang, Experimental investigation of geyser boiling in a two-phase closed loop thermosyphon with high filling ratios, International Journal of Heat and Mass Transfer 127 (2018) 857-869.
[17] Z. Wang, X. Zhao, Z. Han, L. Luo, J. Xiang, S. Zheng, G. Liu, M. Yu, Y. Cui, S. Shittu, M. Hu, Advanced big-data/machine-learning techniques for optimization and performance enhancement of the heat pipe technology – A review and prospective study, Applied Energy 294 (2021).
[18] B. Jiao, L.M. Qiu, Z.H. Gan, X.B. Zhang, Determination of the operation range of a vertical two-phase closed thermosyphon, Heat and Mass Transfer 48(6) (2012) 1043-1055.
[19] C. Huang, W.-K. Lin, S.-R. Wang, Two-Phase Closed-Loop Thermosyphon Solar Water Heater with Porous Wick Structure: Performance and Start-Up Time, Arabian Journal for Science and Engineering 42(11) (2017) 4885-4894.
[20] M. Arab, M. Soltanieh, M.B. Shafii, Experimental investigation of extra-long pulsating heat pipe application in solar water heaters, Experimental Thermal and Fluid Science 42 (2012) 6-15.
[21] W. He, X. Hong, X. Zhao, X. Zhang, J. Shen, J. Ji, Theoretical investigation of the thermal performance of a novel solar loop-heat-pipe façade-based heat pump water heating system, Energy and Buildings 77 (2014) 180-191.

[22] Z. Yang, M. Gong, G. Chen, X. Zou, J. Shen, Two-phase flow patterns, heat transfer and pressure drop characteristics of R600a during flow boiling inside a horizontal tube, Applied Thermal Engineering 120 (2017) 654-671.
[23] K. Kramer, S. Mehnert, K. Geimer, C. Thoma, S. Fahr, P. Ollas, 2.0 GUIDE TO STANDARD ISO 9806:2017 A Resource for Manufacturers, Testing Laboratories, Certification Bodies and Regulatory Agencies, 2018.
[24] H. B. J., L. T. H., H. W. C., S. F. S., Performance evaluation of solar photovoltaic/thermal systems, Solar Energy 70 (2001) 6.
[25] B.J. HUANG;, S.C. Du, A Performance Test Method of Solar Thermosyphon Systems, Journal of Solar Energy Engineering 113 (1991) 8.
[26] X. Ren, J. Li, D. Gao, L. Wu, G. Pei, Analysis of a novel photovoltaic/thermal system using InGaN/GaN MQWs cells in high temperature applications, Renewable Energy 168 (2021) 11-20.
[27] M. Hu, C. Guo, B. Zhao, X. Ao, Suhendri, J. Cao, Q. Wang, S. Riffat, Y. Su, G. Pei, A parametric study on the performance characteristics of an evacuated flat-plate photovoltaic/thermal (PV/T) collector, Renewable Energy 167 (2021) 884-898.
[28] K. Tewari, R. Dev, Exergy, environmental and economic analysis of modified domestic solar water heater with glass-to-glass PV module, Energy 170 (2019) 1130-1150.
[29] A. Shafieian, M. Khiadani, A. Nosrati, A review of latest developments, progress, and applications of heat pipe solar collectors, Renewable and Sustainable Energy Reviews 95 (2018) 273-304.
[30] T. Zhang, Experimental Study on a Forced-Circulation Loop Thermosiphon Solar Water Heating System, International Journal of Photoenergy 2018 (2018) 1-12.